Research Article
Liver Transplantation

JOURNAL
OF HEPATOLOGY

Molecular force-induced liberation of transforming growth factor-beta remodels the spleen for ectopic liver regeneration

Authors

Zhenzhen Wang, Daping Xie, Jiayi Li, …, Peng Zheng, Lei Dong, Chunming Wang

Correspondence

leidong@nju.edu.cn (L. Dong), pengz@nju.edu.cn (P. Zheng), cmwang@umac.mo (C. Wang).

Graphical abstract

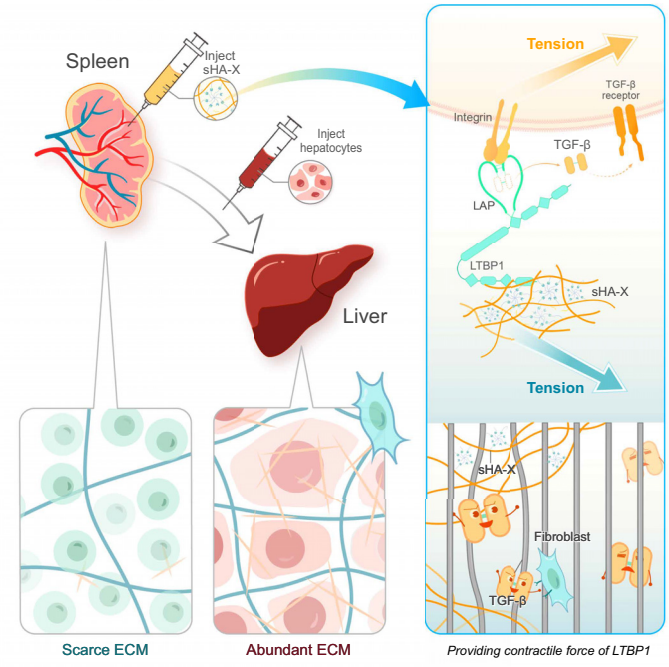

Highlights

- A spleen possesses desirable features for growing a liver, except for the requirement for an ECM-rich matrix.
- The spleen has abundant TGF-β stored in an inactive form that can be activated to remodel the tissue matrix *in situ.*
- sHA-X mechanically liberates TGF-β from the latent complex in the spleen, stimulating collagen production and matrix remodelling.
- The remodelled spleen supports the growth and functions of transplanted liver cells in the spleen.

Impact and implications

Cell transplantation may provide a lifeline to millions of patients with end-stage liver diseases, but their severely damaged livers being unable to accommodate the transplanted cells is a crucial hurdle. Herein, we report an approach to restore liver functions in another organ – the spleen – by activating one single growth factor *in situ*. This approach, based on a chemically designed polysaccharide that can mechanically liberate the active transforming growth factor-β to an unusually high level, promotes the function of abundant allogenic liver cells in the spleen, rescuing animals from lethal models of liver diseases and showing a high potential for clinical translation.

https://doi.org/10.1016/j.jhep.2024.01.005
© 2024 European Association for the Study of the Liver. Published by Elsevier B.V. All rights reserved.

Research Article
Liver Transplantation

JOURNAL
OF HEPATOLOGY

Molecular force-induced liberation of transforming growth factor-beta remodels the spleen for ectopic liver regeneration

Zhenzhen Wang[1,2,†], **Daping Xie**[2,†], Jiayi Li[1], Ziyu Zhai[1], Zhuojian Lu[4], Xuejiao Tian[1], Yiming Niu[2], Qi Zhao[7], Peng Zheng[4,5,*], Lei Dong[1,3,5,*], Chunming Wang[2,6,*]

Journal of Hepatology **2024**. vol. ■ | 1–11

Background & Aims: Ectopic liver regeneration in the spleen is a promising alternative to organ transplantation for treating liver failure. To accommodate transplanted liver cells, the splenic tissue must undergo structural changes to increase extracellular matrix content, demanding a safe and efficient approach for tissue remodelling.
Methods: We synthesised sulphated hyaluronic acid (sHA) with an affinity for the latent complex of transforming growth factor-β (TGF-β) and cross-linked it into a gel network (sHA-X) via click chemistry. We injected this glycan into the spleens of mice to induce splenic tissue remodelling via supraphysiological activation of endogenous TGF-β.
Results: sHA-X efficiently bound to the abundant latent TGF-β in the spleen. It provided the molecular force to liberate the active TGF-β dimers from their latent complex, mimicking the 'bind-and-pull' mechanism required for physiological activation of TGF-β and reshaping the splenic tissue to support liver cell growth. Hepatocytes transplanted into the remodelled spleen developed into liver tissue with sufficient volume to rescue animals with a metabolic liver disorder (*Fah*$^{-/-}$ transgenic model) or following 90% hepatectomy, with no adverse effects observed and no additional drugs required.
Conclusion: Our findings highlight the efficacy and translational potential of using sHA-X to remodel a specific organ by mechanically activating one single cytokine, representing a novel strategy for the design of biomaterials-based therapies for organ regeneration.

© 2024 European Association for the Study of the Liver. Published by Elsevier B.V. All rights reserved.

Introduction

Transforming growth factor-β (TGF-β) plays a pivotal role in tissue development and repair.[1] It stimulates fibroblasts to secrete collagens to construct the extracellular matrix (ECM),[2] regulates immunocytes to induce immunosuppression,[3] and guides cell proliferation, migration, and differentiation.[4] Unlike most other growth factors, TGF-β has a special post-expression control of its extracellular activity.[5] It is secreted from the cell in an inactive latent form, in which the active TGF-β homodimer is wrapped in a large latent complex (LLC) covalently linked to ECM.[6] LLC only releases the active TGF-β upon sensing a proper mechanical[7] or biochemical signal.[8]

This intricate activation mechanism provides a unique possibility to regulate TGF-β activity extracellularly. For example, directly disrupting LLC to liberate TGF-β in the active form can instantly increase the latter's content in the ECM. Since certain tissues store abundant inactive TGF-β while only keeping a small portion activated,[9] liberating stored TGF-β from LLC may unleash its potential to a supraphysiological level, triggering unusually high cellular responses. However, to date, the precise liberation of TGF-β from LLC has not been achieved. Naturally, latent TGF-β can be activated by various pathways,[10,11] and of particular significance is the mode of mechanical activation.[12,13] In LLC, active TGF-β is enveloped by a latency-associated peptide (LAP) linked to latent TGF-β-binding protein-1 (LTBP1).[12,14] On one side, LLC is bound to ECM components such as fibrillin,[15] mediated by interactions between its LTBP1 and glycosaminoglycan (GAG) polysaccharides in the ECM;[16,17] on the other side, LLC can bind to cell-surface integrin receptors (through an Arg-Gly-Asp, or RGD, sequence of LAP).[18] The contractile force collectively generated by these interactions dissociates the complex to release active TGF-β.[19,20] Such *in situ* mechanical activation is specific for TGF-β and more controllable than typical biochemical modes of activation (*e.g.* by proteases or reactive oxygen species).[14,21,22]

A system to mechanically activate TGF-β should mimic ECM by providing i) biochemical affinity for LTBP1 and ii) mechanical

Keywords: Transforming growth factor-β; glycosaminoglycans; biomaterials; liver regeneration; tissue remodelling; hyaluronic acid.
Received 27 August 2023; received in revised form 8 December 2023; accepted 4 January 2024; available online xxx
* Corresponding authors. Addresses: State Key Laboratory of Pharmaceutical Biotechnology, School of Life Sciences, Nanjing University, Nanjing, Jiangsu 210023, China (L. Dong), or State Key Laboratory of Coordination Chemistry, School of Chemistry and Chemical Engineering, Nanjing University, Nanjing, Jiangsu, 210023, China. (P. Zheng), or State Key Laboratory of Quality Research in Chinese Medicine, Institute of Chinese Medical Sciences, University of Macau, Taipa, Macau SAR, China. (C. Wang).
E-mail addresses: leidong@nju.edu.cn (L. Dong), pengz@nju.edu.cn (P. Zheng), cmwang@umac.mo (C. Wang).
† Equal contributions
https://doi.org/10.1016/j.jhep.2024.01.005

support to cooperate with cell-surface integrins in pulling the contractile force on LLC. Since GAG polysaccharides are among the frontline ECM molecules associated with LTBP1 that mediate LLC-ECM interactions,[23] and owing to polysaccharides' favourable physical properties and chemical processability,[24,25] we proposed to develop a glycan biomaterial with the above two key features of ECM. Then, we selected the spleen to test this system, which naturally contains low ECM content[26] and high latent TGF-β storage.[17] We hypothesised that implanting the designed glycan biomaterial in the spleen could efficiently increase local TGF-β activities and radically remodel the splenic tissue matrix, endowing new physiological characteristics to this organ.

To test our hypothesis, we synthesised a sulphated hyaluronic acid (sHA) gel matrix, through LTBP1 affinity screening and click chemistry cross-linking (see graphical abstract). Injecting this system into the mouse spleen sharply increased TGF-β activities *in situ*. Intriguingly, the splenic tissue completely changed from its fluidic nature to a fibrous structure to facilitate liver cell transplants – which hardly settle down in native spleens due to scarce ECM support – to proliferate and exert liver functions.

Materials and methods

The materials and methods used in this study are available in the supplementary materials and CTAT table.

Results

The spleen contains abundant latent TGF-β

To validate the potential of the spleen as the venue for stimulating latent TGF-β activation, we determined the amount of total and active TGF-β in the mouse spleen compared to the liver, which has a highly structured ECM. The ELISA data revealed that the spleen contained over 8,000 pg of total TGF-β per μg of tissue, of which only 25% was active. In contrast, although the liver had a 54% lower storage (about 3,750 pg/μg) of total TGF-β, over 58% was active (Fig. S1A). Immunofluorescence (IF) staining validated that TGF-β in the spleen was mainly co-localised with LTBP1 in the latent form, unlike abundant TGF-β detached from LTBP1 in the liver (Fig. S1B,C).

To examine whether the lack of GAGs accounted for low TGF-β bioavailability in the spleen, we performed GAG ELISA and a dimethyl methylene blue (DMMB) test (Fig. S1D) to quantify GAGs in these two organs. Both assays showed markedly lower (<50%) GAG content in the spleen than in the liver, followed by Alcian blue staining revealing scarce GAGs in the spleen (Fig. S1E). The data illustrated that the mouse spleen contained abundant latent, non-activated TGF-β stored in its GAG-lacking matrix, suggesting the potential for manipulating TGF-β activation.

Synthesised sHAs as GAG mimetic binding to LTBP1

We aimed to design and apply GAG mimetics to trigger a controllable activation of latent TGF-β in the spleen. Major GAG types in the mammalian tissue include heparan sulphate, chondroitin sulphate (CS), dermatan sulphate (DS), and hyaluronic acids (HAs).[27] Since the degree of sulphation is crucial in determining the binding capacity (and thus bioactivity) of GAGs, we chose heparin and HAs – representing the most highly sulphated and non-sulphated GAGs – as the starting materials to synthesise a series of polysaccharides with varying sulphation levels.[25,28] We obtained four sHAs (sHA-1 to -4), with increasing sulphation degrees of 0.08, 1.22, 2.11, and 3.18 from the initial 0.01, and three de-sulphated heparins (DSH-1 to -3), with decreasing sulphation degrees of 0.97, 0.45, and 0.07 from the initial 2.33) (Figs S2 and S3).

Next, we screened these glycans for their binding affinity to the established GAG-binding domain of LTBP1 (SGVHRRR PIHHHVGKGPV),[29,30] using a bio-layer interferometry assay (Fig. 1A). Among these GAGs, sHA-3, with a moderate sulphation degree of 2.11, had a higher binding affinity for LTBP1 than other samples, including the natural CS and DS (Fig. 1B-D). The Kd value of sHA-3 for LTBP1 was quantified as 0.28 nM, verifying their strong affinity (Fig. 1E).

To verify the binding between sHA-3 (denoted as 'sHA' subsequently) and LTBP1 in the complex tissue matrix, we incubated sHA with the spleen homogenate, pulled down the proteins bound to sHA, and observed sHA-enriched LTBP1 with western blotting (Fig. 1F). Moreover, Cy5-labelled sHA was co-localised with LTBP1 in the spleen (Figs 1G and S4), further validating their interaction.

Cross-linked sHA gel (sHA-X) mechanically liberated TGF-β from LLC

To exploit the mechanical force transmitted from the ECM to activate TGF-β, we cross-linked sHA into a gel network via click chemistry (Figs 2A and S5). sHA modified with azide (sHA-PEG_4-N_3) reacted with the DBCO-labelled crosslinker (PEG-8DBCO). The PEG spacer provided a long and flexible connection to minimise steric hindrance involved in its ligation with sHA-N_3, thereby guaranteeing the formation of a cross-linked network (sHA-X), as proven by scanning electron microscope (Fig. 2B). The sHA-X displayed a porous network, with similar pore diameter and porosity to the natural ECM of the decellularised liver tissue (Fig. S6).

To detect whether sHA-X could enhance the mechanical force of the LTBP1-ECM interaction, we employed AFM-SMFS (atomic force microscopy-based single-molecule force spectroscopy)[31,32] to measure the binding strength between LTBP1 and ECM pre-incubated with sHA or sHA-X respectively (Figs 2C and S7). As revealed by the force-extension curves and dissociation force histogram (Fig. 2D,E), ECM with sHA-X had higher interaction forces with LTBP1 (167 pN and 311 pN) than the ECM alone (88 pN and 140 pN) or the ECM with sHA (86 pN). The bivariate density plots in Fig. 2E further illustrated the differences in LTBP1's unfolding characteristics among different groups. These results demonstrated that sHA-X could enhance the mechanical force of LTBP1's interaction with the ECM.

Next, we examined the efficacy of sHA-X in triggering TGF-β release from LLC. To provide the pulling force to LAP, we employed a magnetic field by coating ferromagnetic beads with recombinant integrin αvβ6 – the most potent LAP-binding and TGF-β-activating integrin. The microbeads were adsorbed in the LLC solution bound with sHA or sHA-X. Then, we analysed the activation of LLC under the magnetic force. Once activated, LLC should be disassembled and its constituents (the released active TGF-β in the supernatant, the broken-down LAP attached to the ferromagnetic beads, and LTBP1 adsorbed to sHA-X) should be separately detected (Fig. 2F).

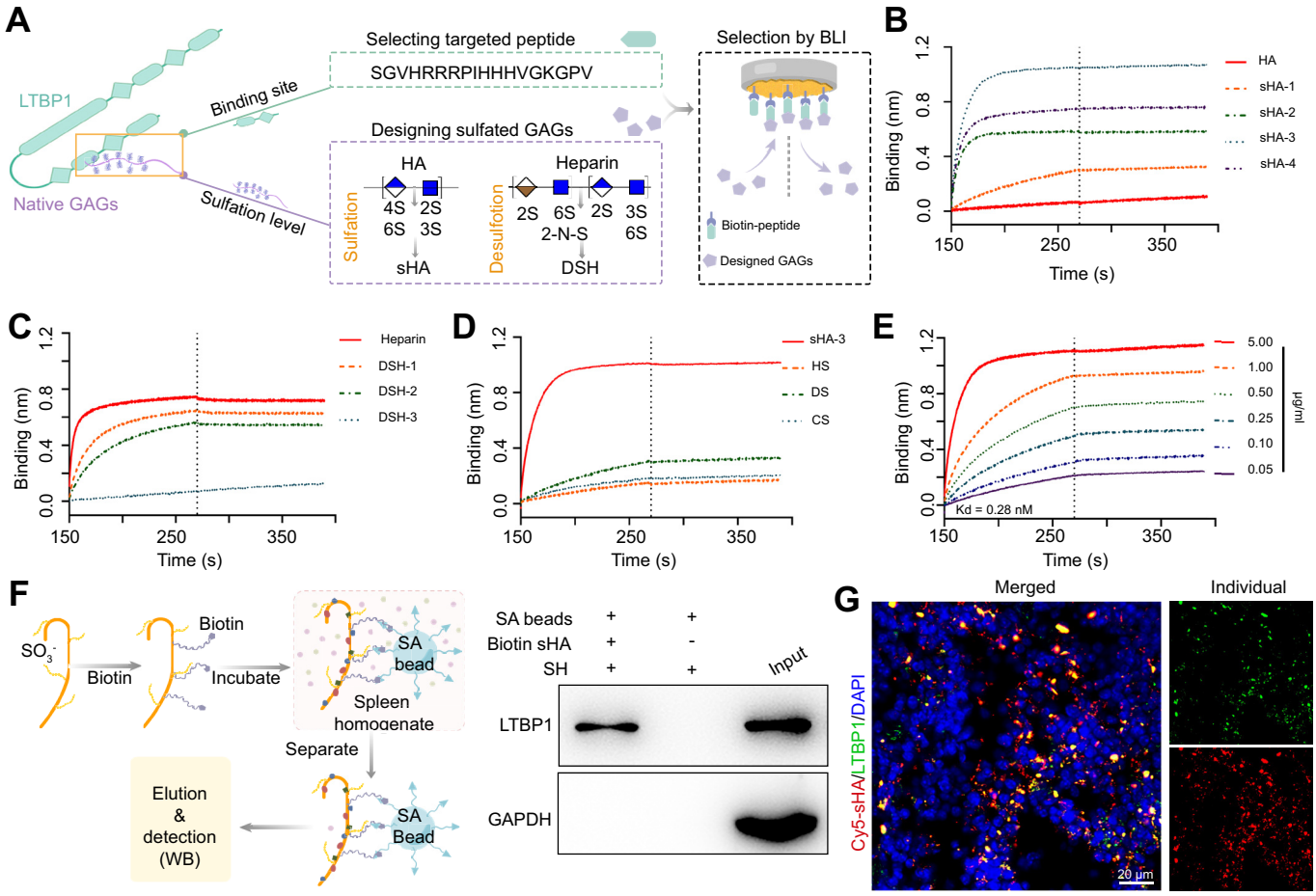

Fig. 1. sHA binds LTBP1 with high affinity. (A) Synthesis and screening of sHA and DSH polysaccharides for their LTBP1-binding affinity; (B-D) BLI analysis of the binding kinetics of (B) HAs with sulphation levels of 0.01, 0.08, 1.22, 2.11 and 3.18 (denoted as HA, sHA-1, sHA-2, sHA-3 and sHA-4); (C) heparin with sulphation degrees of 2.33, 0.97, 0.45 and 0.07 (denoted as heparin, DSH-1, DSH-2 and DSH-3); or (D) other GAGs (HS, CS and DS) to the GAG-binding peptide from LTBP1. (E) The binding kinetics from different concentrations of sHA-3 (denoted as sHA). For (B) to (E), data were fitted with a 1:1 binding model. (F) The method of pulling down proteins in the spleen bound to sHA (left) and WB detection of LTBP1, with GAPDH as a control. (G) Co-localisation of Cy5-labelled sHA (red) and LTBP1 (green) in the spleen after exposure to sHA for 4 h, with DAPI (blue) for nucleus. BLI, bio-layer interferometry; DS, dermatan sulphate; DSH, de-sulphated heparin; Fah, fumarylacetoacetate hydrolase; GAG, glycosaminoglycan; HAs, hyaluronic acids; HS, heparan sulphate; ICG, indocyanine green; LTBP1, latent TGF-β-binding protein-1; sHA, sulphated hyaluronic acid; WB, western blotting.

Based on this method, we determined the active TGF-β in the supernatant by ELISA and detected the proteins on beads and in the pellets with SDS-PAGE. Following the pulling of the αvβ6 integrin-coated beads, the active TGF-β was abundantly present in the supernatant of the sHA-X group, with a significantly higher (~20 fold) bioavailability than that in the sHA group, reaching 40% of total TGF-β (Fig. 2G). Consistently, Coomassie's brilliant blue staining illustrated LTBP1 and LAP bound onto the biomaterials and beads, respectively, in the sHA-X group; in contrast, LLC remained largely intact in the sHA group (Fig. 2H).

We further verified the effectiveness of sHA-X in mechanically activating TGF-β by employing a reporter cell line HEK293-$_{(CAGA12\text{-}Luc)}$,[33] which stably expresses TGF-β-sensitive luciferase (Fig. 2I). Stimulated by thrombin to trigger the pulling force of cellular integrin to LAP,[34,35] LLC incubated with sHA-X freed significantly more active TGF-β (~40-fold higher luciferase activity) than that from the sHA group (Fig. 2J). Consequently, the level of phosphorylated Smad2/3, a major operator of the TGF-β signalling pathway, in the sHA-X group was found to be comparable to that in the positive control (treated with active TGF-β) and higher than that in the sHA group (Figs 2K and S8), highlighting the successful liberation of active TGF-β from its latent complex.

sHA-X liberated TGF-β in the mouse spleen

To test whether sHA-X could liberate endogenous TGF-β from LLC *in vivo*, we injected this biomaterial into the translocated mouse spleen.[26] Briefly, the spleen was surgically moved from the inner abdomen to a subcutaneous site, remaining blood vessels connected to other organs (Fig. S9A,B and Video S1), as further confirmed by MRI (Fig. S9C). The translocated spleen maintained its vasculature (blood flow, haemoglobin content, structure and distribution; Fig. S10) and ECM (collagen; Fig. S11). Scanning electron microscope images revealed that the injected sHA-X displayed a porous network, distributed uniformly in the native and decellularised splenic space (Fig. 2L), compensating for the ECM that was naturally lacking in this organ. Using Cy5-labelled sHA, we observed that sHA-X generated the desirable microstructure, while uncrosslinked

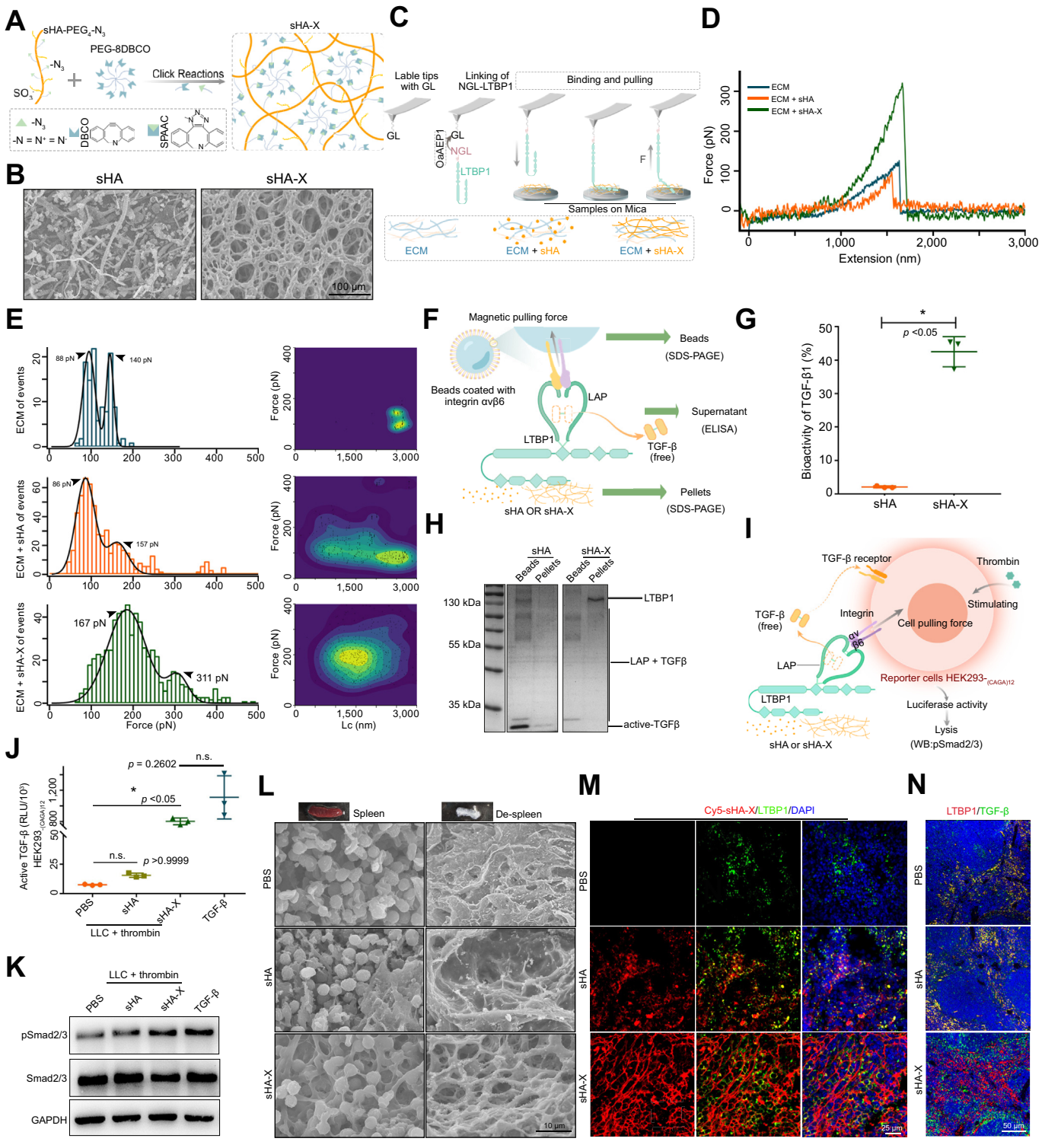

Fig. 2. sHA-X network induces TGF-β release from LLC. (A). Preparation of the sHA-X via click chemistry. (B) SEM images of sHA and sHA-X. (C) Single-molecule mechanics' assay based on AFM measurement to quantify the strength between LTBP1 and sHA or sHA-X on the decellular spleen tissue. (D) Representative force-extension curves show specific binding events between LTBP1 with sHA or sHA-X. (E) Summarised histograms of ΔLc values in frequency (left) and ΔLc-force pairs for every individual unfolding event plotted in bivariate colour-coded density plots (right). In the histograms, the fitted curve of event populations was shown in black lines; arrowheads indicate population maxima; In the bivariate density maps, blue represents the low and yellow high frequency of events. (F) The procedure to mimic TGF-β release from LLC under mechanical stimulation provided by ferromagnetic microbeads coated with LAP-binding recombinant integrin αvβ6 *in vitro*. (G) The TGF-β bioactivity of supernatant in sHA or sHA-X group treated as in panel F, measured by ELISA. (H) Coomassie brilliant blue R250 staining images of proteins adsorbed on the beads or detained in the pellets treated as in panel F after SDS-PAGE. (I–K) The schematic diagram, the luciferase intensity and western blotting analysis of the cellular experiment to detect active TGF-β released from LLC, based on a TGF-β-sensitive reporter cell (HEK293-$_{(CAGA)12}$). (L) SEM images of the spleen or the

sHA was randomly dispersed in the tissue (Fig. 2M). Biodistribution tests showed the stable retention of sHA-X in the spleen (Fig. S12), which was favourable for prolonging its interaction with LTBP1, in contrast to the significant diffusion of non-cross-linked sHA from the spleen to other organs. Encouragingly, co-staining for LTBP1 indicated that the injected sHA-X immobilised the endogenous LTBP1 into its network in the spleen, proving that sHA-X took up the role of a mechanically supportive ECM. Meanwhile, IF staining illustrated the separation of TGF-β and LTBP1 in the tissue injected with sHA-X (Figs 2N and S13). Meanwhile, ELISA results indicated a rapid increase in TGF-β bioavailability from ∼20% to ∼60% within 1 day (Fig. S14), without affecting TGF-β concentrations in the serum (Fig. S15), reflecting the precise modulation and scarce systemic response. Further examinations, including histological imaging, blood routine index, blood pressure analysis, serum biochemical factors, and blood flow tests, revealed no abnormalities and validated the safety of this biomaterial (Fig. S16, Table S1-3). These data provided multi-angle evidence that sHA-X successfully liberated TGF-β *in situ*.

Supplementary video related to this article can be found at https://doi.org/10.1016/j.jhep.2024.01.005.

sHA-X remodelled the spleen matrix through fibroblast activation

We then performed multiple injections of this biomaterial for indicated times to remodel the spleen according to reported literature (Fig. 3A).[36] The Masson's trichrome staining results suggested that ECM increased along with the injections (Fig. S17), and the hydroxyproline in the spleen increased significantly after four-time injections (Fig. 3B).

Injections of sHA-X markedly reshaped the gross structure and microstructure of spleen tissue. First, the sHA-X-remodelled spleens increased in size and weight to twice that of the PBS-treated group (Fig. 3C). Second, H&E staining illustrated that (Fig. 3D), after remodelling, the typical splenic structure of red and white pulps disappeared, the density of lymph cells decreased, and the deposition of matrix increased. Third, Masson's trichrome staining revealed an elevated density of tissue matrix (Fig. 3E), particularly collagens, in the remodelled spleen.

We observed dramatically increased and activated mesenchymal cells in the sHA-X group. The vimentin$^+$ cells in the remodelled spleen accounted for 38.8% of the non-immunocytes (CD45$^-$), twice that in the PBS group (Figs 3F and S18). Besides, these vimentin$^+$ cells were dramatically activated (α-SMA$^+$; Fig. 3G). Further, the spleen remodelled by sHA-X contained ∼7.12% splenic reticular fibroblasts labelled with gp38 in the total splenocyte, around 3.5-fold higher than in the PBS group (Figs 3H and S19). The splenic reticular fibroblasts labelled with the specific marker (ER-TR7) were significantly activated (Fig. 3I). Consequently, under sHA-X treatment, the spleens displayed a remarkable increase in the content of type I and type IV collagen (Figs 3J and S20). These data indicated the role of fibroblasts in driving the remodelling.

Next, to better understand the biological changes in the sHA-X-remodelled spleen, we employed a PCR array to analyse ECM- and cell adhesion-related molecules at the transcriptional level. The heatmap showed that the majority of 26 kinds of ECM-associated genes were significantly upregulated in the sHA-X group, similar to the treatment of soluble TGF-β, confirming a thorough remodelling of the spleen (Fig. 3K). However, the change could be dramatically abolished by a TGF-β inhibitor (SB431542), indicating the central role of TGF-β activation underlying the effect of sHA-X.

In addition to activating fibroblasts, TGF-β is also known for its immunosuppressive functions. Immunocyte profiling demonstrated a marked decrease in the natural killer cells (CD49 b$^+$), macrophages (F4/80$^+$) and T cells (CD4$^+$ or CD8$^+$) (Fig. S21), together with the elevated secretion of the anti-inflammatory factor IL-10 (Fig. S22). These changes represented the creation of an immunosuppressive microenvironment in the sHA-X-remodelled spleen.

We further demonstrated that remodelling the spleen in immunodeficient NCG-X mice with T, B and NK cell deficiency[37] still facilitated desirable settlement of the transplanted hepatocytes (Fig. S23), proving the indispensability of ECM remodelling.

The above findings demonstrated that, through *in situ* liberation of TGF-β, the sHA-X matrix effectively activated fibroblasts and increased collagen deposition, radically remodelling the splenic matrix into an ECM-rich microenvironment.

Transplanted hepatocytes grew in the sHA-X-remodelled spleen

We evaluated whether the remodelled spleen could support the settlement of transplanted liver cells, which need to adhere to a collagenous ECM structure for growth. Flow cytometry analysis identified 12.1% GFP-labelled allogeneic primary hepatocytes among non-immunocytes (CD45$^-$) in the sHA-X-remodelled spleen 24 h post-inoculation, over twice that of the PBS group (Figs 4A and S24). Consistently, more GFP-labelled hepatocytes were presented in the sHA-X group (Fig. 4B,C). The H&E staining and EdU co-staining with GFP showed that the transplanted hepatocytes steadily proliferated through 30 days in the sHA-X-remodelled spleen but mostly disappeared in the PBS-treated group (Figs 4D and S25). The GFP-positive hepatocytes reached 11.9% of the total splenic cells in the remodelling group but only 4.04% in the PBS group (Fig. 4E). After 30 days of transplantation, the sHA-X-remodelled spleen contained densely arrayed polygonal hepatocytes, occupying most of the tissue space (Fig. 4F), while scarce hepatocytes emerged in the PBS group. Additionally, the sHA-X-remodelled spleen highly expressed metabolic enzymes CYP1A2 and albumin (Fig. 4G), two key markers of liver parenchymal cells, indicating the satisfactory growth of hepatocytes therein.

The transplanted hepatocytes displayed their phenotypes. Apart from positive staining of CYP1A2 and albumin, and the proliferation marker EdU (Fig. 4H), they formed an appropriate hepatic structure, reflecting liver zonation and bile ducts,

decellularised spleen tissue exposed to sHA or sHA-X for 4 h, with PBS group as control. (M) The immunofluorescence images to show the distribution of Cy5-labelled sHA and sHA-X (red, right column) and their co-localisation with LTBP1 (green, middle column) in the spleen treated as in panel L. (N) The distribution of LTBP1 and TGF-β in the spleen exposed to sHA or sHA-X for 24 h. Images are representative of three independent experiments. Results are shown as mean ± SD. Significant differences were determined by Student's *t* test or one-way ANOVA with *Tukey*'s multiple-comparison *post hoc* test. LLC, large latent complex; LAP, latency-associated peptide; LTBP1, latent TGF-β-binding protein-1; sHA, sulphated hyaluronic acid; sHA-X, cross-linked sHA network; TGF-β, transforming growth factor-β.

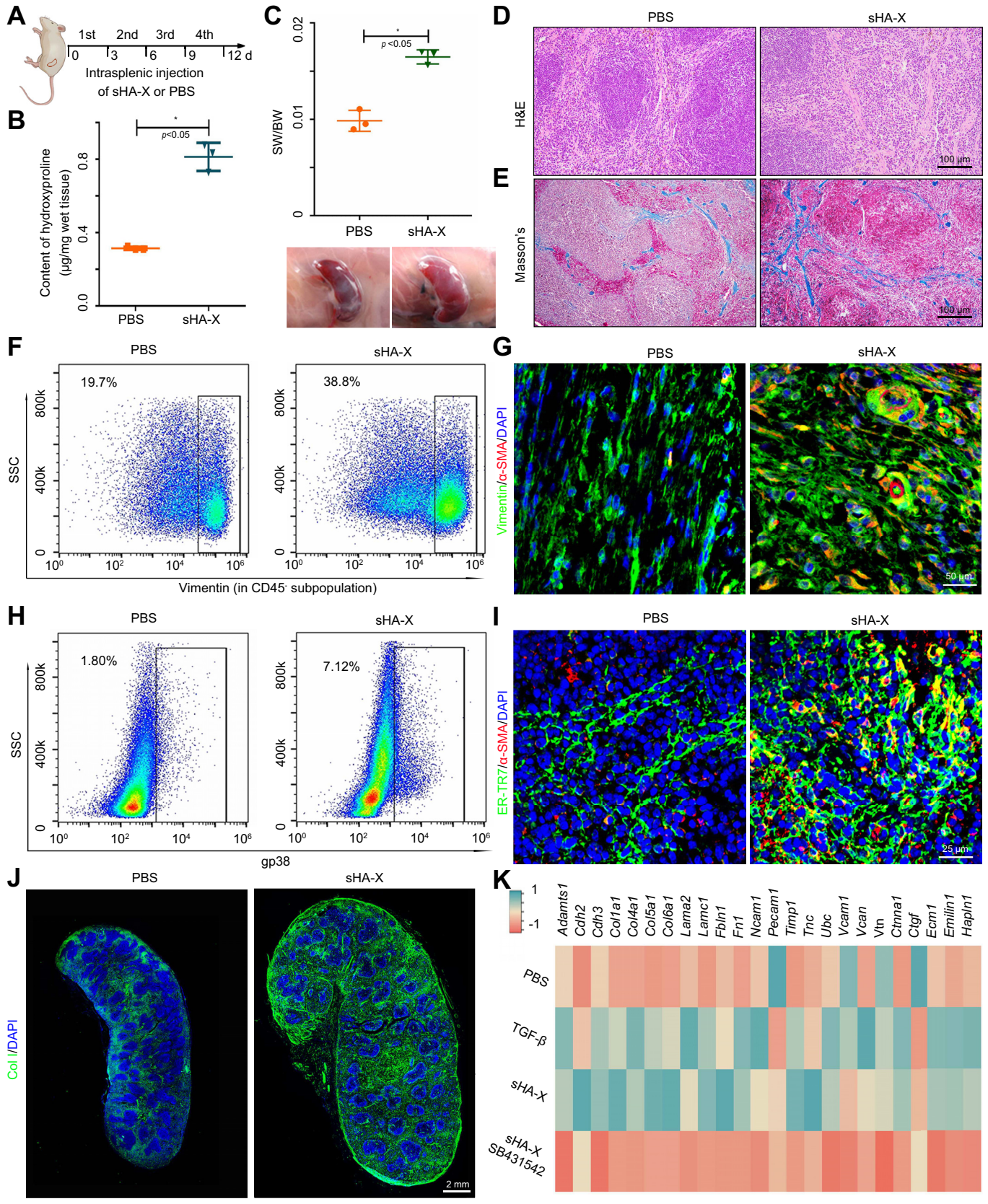

Fig. 3. sHA-X remodels the spleen matrix. (A) The schedule of intrasplenic injection of sHA-X every 4 days for spleen remodelling, with PBS treatment as control. (B) The content of hydroxyproline in PBS-treated spleen and sHA-X-remodelled spleen normalised to wet tissue after injection four times. (C) The weight of the spleen exposed to sHA-X four times normalised to body weight, with the spleen morphology shown beneath. (D-E) H&E and Masson's trichrome staining of spleen treated as in panel B. (F-G) Representative flow cytometry (vimentin) and immunofluorescence images of (Vimentin: green, α-SMA: red) mesenchymal cells in the spleens treated

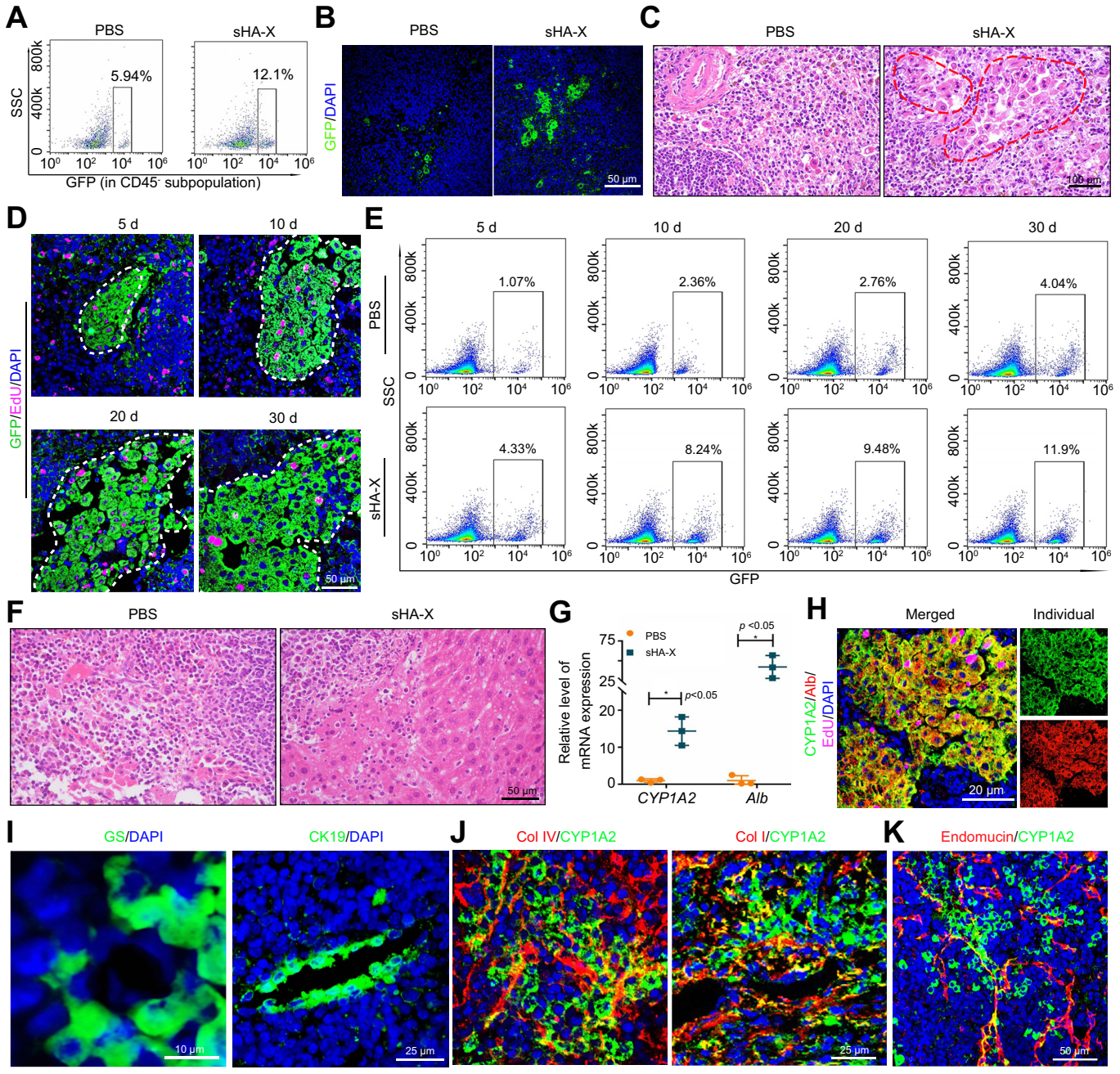

Fig. 4. The sHA-X-remodelled spleen supports hepatocyte transplants. (A-C) Flow cytometry (A), fluorescence (B) and H&E staining (C) images of GFP-labelled hepatocytes in PBS-treated or sHA-X-remodelled spleens 1 day after the implantation of primary hepatocytes, with hepatocytes circled in red dotted lines in (C). (D) GFP-hepatocytes in the spleen at indicated (5, 10, 20, and 30) days after injection into sHA-X-remodelled spleens, with the EdU staining (magenta) to show the proliferation. The white dotted lines showed the distribution of hepatocytes. (E) Flow cytometry of GFP-hepatocytes in the spleen treated as in panel D. (F) H&E staining for hepatocytes in the sHA-X-remodelled spleen at 30 days after implantation, with hepatocytes circled in red dotted lines. (G) Gene expression of typical hepatocyte marker (CYP1A2 and Alb) in the spleen treated as in panel F. (H) The IF co-staining of EdU with hepatic markers (CYP1A2, Alb) in the spleen treated as in panel F. (I) Staining for GS (liver zonation) and CK19 (bile duct). (J-K) Co-immunofluorescence staining of Col4, Col1 (J), and endomucin (K) (red) with hepatocyte markers CYP1A2 (green) to analyse the integration of ECM or blood vessels with hepatocytes. Images are representative of three independent experiments. Results are shown as mean ± SD. Significant differences were determined by two-way ANOVA with *Tukey*'s multiple-comparison *post hoc* test. ECM, extracellular matrix; IF, immunoflourescence; sHA, sulphated hyaluronic acid; sHA-X, cross-linked sHA network.

as in panel B. (H–I) Representative flow cytometry (gp38) and immunofluorescence images (ER-TR7: green, α-SMA: red) of splenic reticular fibroblasts in the spleens treated as in panel B. (J) Distribution of Col1 in the whole spleen sections; (K). Heatmap of ECM-related genes expressed by PBS-treated spleen, TGF-β-treated spleen, or sHA-X-remodelled spleen. For the inhibition group (sHA-X/SB431542), the spleen was exposed to sHA-X, following the stimulation of the inhibitor SB431542 of TGF-β receptor for 30 min. Results are shown as mean ± SD. Significant differences were determined by the Student's *t* test. ECM, extracellular matrix; sHA, sulphated hyaluronic acid; sHA-X, cross-linked sHA network; TGF-β, transforming growth factor-β.

as demonstrated by IF staining for glutamine synthetase (GS) and the typical bile duct marker CK19 (Fig. 4I). Essentially, the key hepatic supportive microstructures, including collagens and blood vessels, were enriched around the hepatocytes (Fig. 4J,K), further indicating a desirable settlement of hepatocytes. These data highlighted that the sHA-X-remodelled spleen supported the settlement and growth of transplanted liver cells.

Transplanted hepatocytes in the sHA-X-remodelled spleen performed liver functions

Finally, we evaluated whether these transplanted hepatocytes could perform proper physiological functions of the liver.

First, microarray analysis indicated the expression of genes responsible for hepatic functions in the sHA-X-remodelled spleen (Fig. 5A). Also, the hepatised spleen synthesised glucose and lipids, as demonstrated by periodic acid-Schiff and Oil Red O staining, respectively (Fig. 5B). Further, after ligating the hepatic portal vein and hepatic artery to exclude the interference of the host liver, we performed the absorption and clearance test of indocyanine green (ICG), and drug metabolism analysis of CYP1A2 for assessing the functions of the transplanted liver cells (Fig. 5C). Observation of ICG in frozen sections and the ICG retention rate at 15 min (ICG_{R15}) data illustrated that the hepatised spleens developed the uptake capacity of the liver (Fig. 5D,E). Then, after the same ligation, we injected phenacetin and tested the enzymatic activities of cytochrome P450 in the PBS-treated or sHA-X-remodelled spleen. A high serum level of acetaminophen, the specific liver metabolite, in mice with the hepatised spleen suggested they developed metabolic functions via the transplanted hepatocytes (Fig. 5F).

Then, we evaluated the capacity of the hepatic spleen to compensate for the native liver functions in two extreme models: i) metabolically deficient transgenic mice[38] and ii) mice with 90% hepatectomy.[36] In the first model we used fumarylacetoacetate hydrolase-knockout (*Fah*$^{-/-}$) mice, which normally die as neonates with severe hepatic dysfunction and rely upon 2-(2-nitro-4-trifluoro-methylbenzyol)-1,3-cyclohexanedione (NTBC) supply (Fig. 5G). All the *Fah*$^{-/-}$ mice after NTBC withdrawal (*Fah*$^{-/-}$$_{NTBC\text{-}off}$) in the PBS group died within 7 weeks and showed continuous loss of body weight (Figs 5H and S26A); in contrast, 75% *Fah*$^{-/-}$$_{NTBC\text{-}off}$ mice with hepatised spleens were alive after more than 12 weeks, while maintaining body weight. These results indicated that hepatised spleens could repopulate and rescue *Fah*$^{-/-}$$_{NTBC\text{-}off}$ mice. Moreover, serum levels of tyrosine and phenylalanine were markedly reduced in mice with hepatised spleen, comparable to the *Fah*$^{-/-}$ mice maintained with NTBC (NTBC group) (Fig. 5I). Similarly, these mice also showed decreased levels of aspartate aminotransferase, alanine aminotransferase, total bilirubin, blood urea nitrogen and creatinine (Figs 5J and S26B), indicating that the hepatised spleen alleviated liver and other organ injury.

In the second model of 90% hepatectomy (Figs 5K and S27), all mice with the hepatised spleen – but none in the PBS group – survived within 48 h post-surgery (Fig. 5L). Meanwhile, through the 14-day observation, hepatectomy sharply increased blood ammonia and decreased blood glucose levels, which were quickly controlled by day 2 and returned to normal by day 8 in the mice with hepatised spleens, while the mice in the PBS group died within 48 h (Fig. 5M).

Discussion

In this study, we have demonstrated an engineering approach for instantly increasing local TGF-β activity, which completely reshaped the fluidic state of the native spleen into a fibrotic matrix to support the growth of transplanted liver cells. Unlike all existing approaches, our strategy targets the unique mechanism of TGF-β activation. The designed LTBP1-binding, cross-linked matrix provided the mechanical force required to liberate this multipotent growth factor from its latent complex, without introducing exogenous genes or proteins – and the whole process was completed locally and extracellularly. Because of the abundant storage of the inactive complex in the spleen,[11] such activation could efficiently reach a maximal magnitude. The unleashed endogenous TGF-β activity adequately activated splenic fibroblasts to proliferate and produce abundant collagens, eventually establishing a microenvironment favourable for the ectopic growth of hepatocytes. These outcomes reveal the underappreciated potential of activating existing growth factors for endogenously driven tissue regeneration.

We selected GAGs as the starting material to design this matrix, based on their biochemical role in TGF-β activation. GAGs provide essential anchoring sites for the LTBP1-ECM interaction.[23,25] After synthesising GAGs of various sulphation degrees and structures, we compared their LTBP1-binding capacity and identified sHA-3 with a desirable binding affinity (higher than DS and CS) and specificity.[39] Notably, the mechanical resistance of LTBP1 to the cellular pulling force is crucial for triggering TGF-β release, and this force is transmitted through LTBP1 to the ECM via GAGs. Without this force, the non-cross-linked sHA molecules – only providing the affinity but not the mechanical force – failed to trigger TGF-β release. The cross-linked sHA-X system fulfilled the expectation because it integrated the biochemical affinity of GAGs and the mechanical support of the ECM.

Our investigation further highlights the spleen as a transformable organ for liver regeneration, in agreement with previous explorations by us and others.[26,36,40] Its advantages for accommodating a high number of transplanted cells include a large volume, rich vasculature, and physiological connection with the liver,[41] but it has an extremely loose tissue structure with scarce ECM,[42] which does not support the cell adherence that is crucial for hepatocyte survival.[43,44] Accordingly, we harnessed the prominent role of TGF-β to drive ECM formation. The translational value of this approach is highlighted by the superior liver function of the hepatised spleen in both the metabolic liver disorder model (*Fah*$^{-/-}$ model)[38] and hepatectomy model (90% hepatectomy).[36] They could prolong the survival time by up to 40%. Successful restoration of liver functions in these challenging models rigorously validated the efficacy of our strategy, which may open a new avenue for growing one tissue from another of distinct nature by precisely manipulating one single growth factor extracellularly.

Future studies will focus on safety assessment and extended applications of this technology in more clinically relevant scenarios. Although the developed polysaccharide

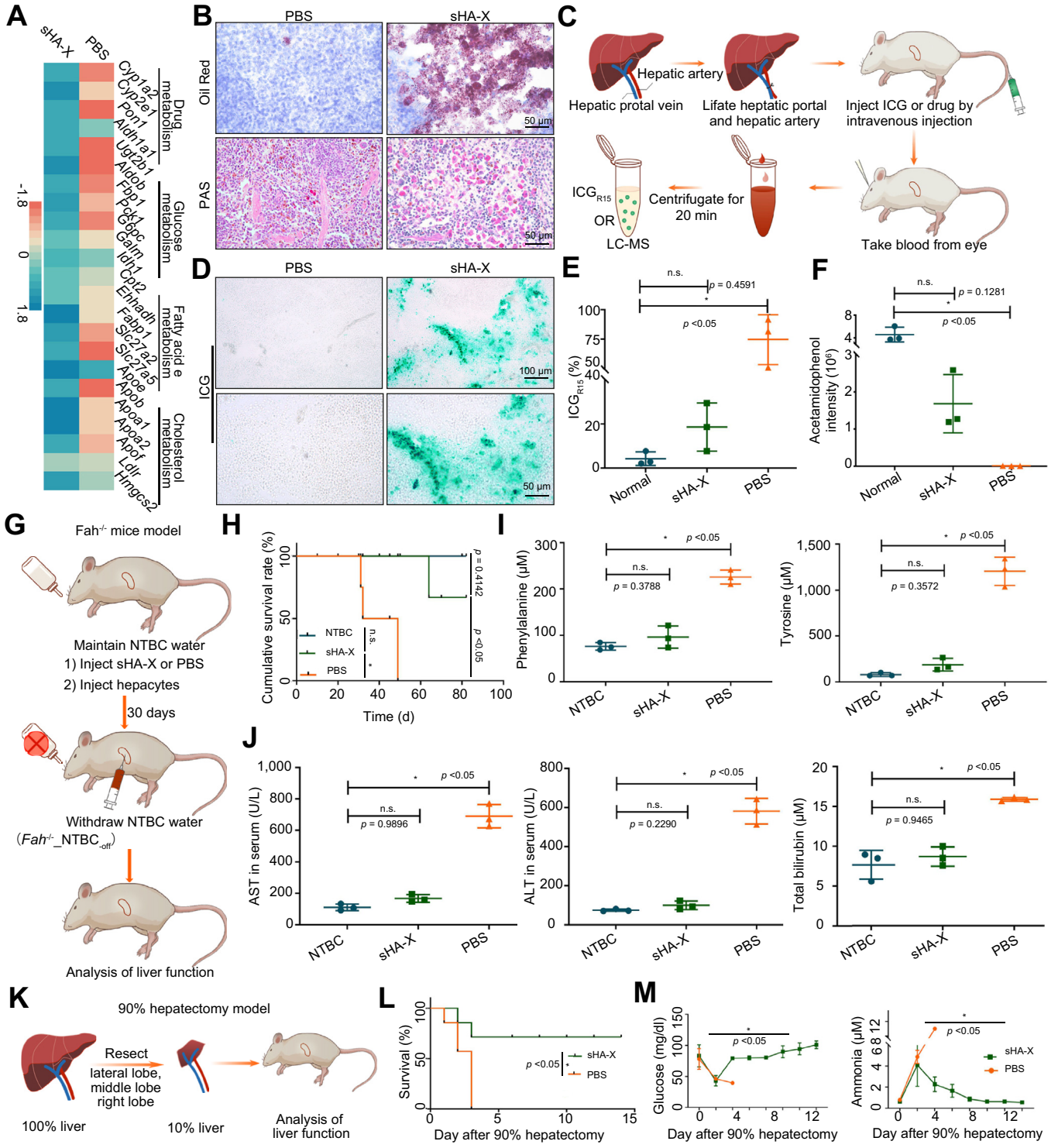

Fig. 5. The sHA-X-remodelled spleen implanted with hepatocytes performs essential liver functions. (A) Microarray analysis of hepatocyte gene expression associated with metabolism in the PBS-treated and sHA-X-remodelled spleens 30 days after the implantation of primary hepatocytes. Three tissue samples from each independent experiment were pooled. (B) Oil Red O and PAS staining in the spleens treated as in panel A. (C) The schematic diagram of the experiment of ICG_{R15} and drug metabolism assay. (D-F) ICG uptake (D), ICG clearance analysis (E) and CYP450 metabolic activity test (F) were performed as in panel C. (G) Schematic outline of primary hepatocyte transplantation into PBS-treated, or sHA-X-remodelled spleen of *Fah*$^{-/-}$_NTBC-off mice, with the *Fah*$^{-/-}$ model maintaining with NTBC water (NTBC group) as control. (H) The survival curve of NTBC group, or *Fah*$^{-/-}$_NTBC-off mice treated as in panel G (n = 7). (I-J) Serum levels of phenylalanine, tyrosine (I), AST, ALT, and total bilirubin (J) in NTBC group, or *Fah*$^{-/-}$_NTBC-off mice at 30 days treated as in panel G. (K) Illustration of murine 90% hepatectomy. (L-M) Survival curve (L, n = 7), and glucose and ammonia levels (M) in 90% hepatectomised mice after the implantation of primary hepatocytes into PBS-treated or sHA-X-remodelled spleens for 30 days. Images are representative of three independent experiments. Results are shown as mean ± SD. Significant differences were determined by one-way ANOVA with Tukey's multiple-comparison *post hoc* test or repeated measures ANOVA test with *post hoc Bonferroni* correction. The survival curve significance was determined by log-rank (Mantel-Cox) test. ICG, indocyanine green; NTBC, 2-(2-nitro-4-trifluoro-methylbenzyol)-1,3-cyclohexanedione; PAS, periodic acid-Schiff; sHA, sulphated hyaluronic acid; sHA-X, cross-linked sHA network.

biomaterial may be degradable by hyaluronidases and showed no adverse responses, a long-term observation of its *in vivo* fate will benefit future translation. Also, certain liver diseases, such as hepatitis and cirrhosis, might cause splenic abnormalities, it is worth exploring how this system works under such pathological conditions.

Affiliations

[1]*State Key Laboratory of Pharmaceutical Biotechnology, School of Life Sciences, Nanjing University, Nanjing, Jiangsu 210023, China;* [2]*State Key Laboratory of Quality Research in Chinese Medicine, Institute of Chinese Medical Sciences, University of Macau, Taipa, Macau SAR, China;* [3]*National Resource Center for Mutant Mice, Nanjing, Jiangsu, 210023, China;* [4]*State Key Laboratory of Coordination Chemistry, School of Chemistry and Chemical Engineering, Nanjing University, Nanjing, Jiangsu, 210023, China;* [5]*Chemistry and Biomedicine Innovative Center, Nanjing University, Nanjing, Jiangsu 210023, China;* [6]*Department of Pharmaceutical Sciences, Faculty of Health Science, University of Macau, Taipa, Macau SAR, China;* [7]*Department of Biomedical Sciences, Faculty of Health Science, University of Macau, Taipa, Macau SAR, China*

Abbreviations

ALT, alanine aminotransferase; AST, aspartate aminotransferase; CS, chondroitin sulphate; DS, dermatan sulphate; DSHs, de-sulphated heparins; ECM, extracellular matrix; *Fah*, fumarylacetoacetate hydrolase; GAG, glycosaminoglycan; HAs, hyaluronic acids; ICG, indocyanine green; LLC, large latent complex; LAP, latency-associated peptide; LTBP1, latent TGF-β-binding protein-1; NTBC, 2-(2-nitro-4-trifluoro-methylbenzyol)-1,3-cyclohexanedione; sHA, sulphated hyaluronic acid; sHA-X, cross-linked sHA network; TGF-β, transforming growth factor-β.

Financial support

This study was financially supported by a jointly sponsored project between the National Science Foundation of China (NSFC, No. 31961160701; to L.D.) and the Science and Technology Development Fund, Macao SAR (FDCT, No. 0018/2019/AFJ; to C.W.). It was also supported by grants from NSFC (32022088, 31971309, 32001069, 32370839, and 32230056), FDCT (No. 0001/2021/AKP and 0060/2020/AGJ), the Natural Science Foundation of Jiangsu Province (BK20200318), and the University of Macau (MYRG2022-00100-ICMS).

Conflict of interest

The authors declare no potential conflicts of interest.

Please refer to the accompanying ICMJE disclosure forms for further details.

Authors' contributions

L.D. and C.W. conceived the study. Z.W. designed and performed major chemical and biological experiments. D.X. designed and performed chemical synthesis. C.W., L.D., and Z.W. drafted the manuscript. Z.Z., J.L., Z.L., Y.N., and X.T. contributed to biological experiments and data analysis. P.Z. contributed to biomechanics assays. Q.Z. contributed to biochemical assays. L.D. and C.W. provided funding support. All authors contributed to manuscript writing and proofreading.

Data availability statement

The data generated in this study are available within the article and its supplementary data files. Additional data related to this paper are available upon reasonable request from the corresponding authors.

Acknowledgements

The authors thank Dr Lin Song and Dr Chunyan Liu for their technical help in establishing the animal model.

Supplementary data

Supplementary data to this article can be found online at https://doi.org/10.1016/j.jhep.2024.01.005.

References

Author names in bold designate shared co-first authorship

[1] Siegel PM, Massagué J. Cytostatic and apoptotic actions of TGF-β in homeostasis and cancer. Nat Rev Cancer 2003;3:807–820.
[2] Meng X, Nikolic-Paterson DJ, Lan H. TGF-β: the master regulator of fibrosis. Nat Rev Nephrol 2016;12:325–338.
[3] Batlle E, Massagué J. Transforming growth factor-β signaling in immunity and cancer. Immunity 2019;50:924–940.
[4] Zhang Y, Alexander PB, Wang XF. TGF-β family signaling in the control of cell proliferation and survival. Cold Spring Harbor Perspect Biol 2017;9.
[5] Miyazono K, Olofsson A, Colosetti P, et al. A role of the latent TGF-beta 1-binding protein in the assembly and secretion of TGF-beta 1. EMBO J 1991;10:1091–1101.
[6] Horiguchi M, Ota M, Rifkin DB. Matrix control of transforming growth factor-beta function. J Biochem 2012;152:321–329.
[7] Liénart S, Merceron R, Vanderaa C, et al. Structural basis of latent TGF-β1 presentation and activation by GARP on human regulatory T cells. Science 2018;362:952–956.
[8] Ge G, Greenspan DS. BMP1 controls TGFbeta1 activation via cleavage of latent TGFbeta-binding protein. J Cel Biol 2006;175:111–120.
[9] Khan SA, Joyce J, Tsuda T. Quantification of active and total transforming growth factor-β levels in serum and solid organ tissues by bioassay. BMC Res Notes 2012;5:636.
[10] Shi M, Zhu J, Wang R, et al. Latent TGF-β structure and activation. Nature 2011;474:343–349.
[11] Evrard S, Bluteau O, Tulliez M, et al. Thrombospondin-1 is not the major activator of TGF-β1 in thrombopoietin-induced myelofibrosis. Blood 2011;117:246–249.
[12] Wipff P-J, Rifkin DB, Meister J-J, et al. Myofibroblast contraction activates latent TGF-β1 from the extracellular matrix. J Cel Biol 2007;179:1311–1323.
[13] Zhen G, Guo Q, Li Y, et al. Mechanical stress determines the configuration of TGFβ activation in articular cartilage. Nat Commun 2021;12:1706.
[14] **Dong X**, **Zhao B**, Iacob RE, et al. Force interacts with macromolecular structure in activation of TGF-β. Nature 2017;542:55–59.
[15] Isogai Z, Ono RN, Ushiro S, et al. Latent transforming growth factor beta-binding protein 1 interacts with fibrillin and is a microfibril-associated protein. J Biol Chem 2003;278:2750–2757.
[16] Zollinger AJ, Smith ML. Fibronectin, the extracellular glue. Matrix Biol 2017;60–61:27–37.
[17] Robertson IB, Rifkin DB. Regulation of the bioavailability of TGF-β and TGF-β-related proteins. Cold Spring Harbor Perspect Biol 2016;8.
[18] Annes JP, Chen Y, Munger JS, et al. Integrin αVβ6-mediated activation of latent TGF-β requires the latent TGF-β binding protein-1. J Cel Biol 2004;165:723–734.
[19] Keski-Oja J, Koli K, von Melchner H. TGF-beta activation by traction? Trends Cel Biol 2004;14:657–659.
[20] Hinz B. The extracellular matrix and transforming growth factor-beta1: tale of a strained relationship. Matrix Biol 2015;47:54–65.
[21] Jenkins G. The role of proteases in transforming growth factor-β activation. Int J Biochem Cel Biol 2008;40:1068–1078.
[22] Noskovicova N, Schuster R, van Putten S, et al. Suppression of the fibrotic encapsulation of silicone implants by inhibiting the mechanical activation of pro-fibrotic TGF-beta. Nat Biomed Eng 2021;5:1437–1456.
[23] Chen Q, Sivakumar P, Barley C, et al. Potential role for heparan sulfate proteoglycans in regulation of transforming growth factor-beta (TGF-beta) by modulating assembly of latent TGF-beta-binding protein-1. J Biol Chem 2007;282:26418–26430.
[24] Palhares L, London JA, Kozlowski AM, et al. Chemical modification of glycosaminoglycan polysaccharides. Molecules 2021;26.
[25] Bishop JR, Schuksz M, Esko JD. Heparan sulphate proteoglycans fine-tune mammalian physiology. Nature 2007;446:1030–1037.
[26] **Wang L**, **Wang C**, Wang Z, et al. Transforming the spleen into a liver-like organ in vivo. Sci Adv 2020;6:eaaz9974.
[27] Kang Z, Zhou Z, Wang Y, et al. Bio-based strategies for producing glycosaminoglycans and their oligosaccharides. Trends Biotechnol 2018;36:806–818.
[28] Karlsson R, Chopra P, Joshi A, et al. Dissecting structure-function of 3-O-sulfated heparin and engineered heparan sulfates. Sci Adv 2021;7:eabl6026.
[29] Annes JP, Chen Y, Munger JS, et al. Integrin alphaVbeta6-mediated activation of latent TGF-beta requires the latent TGF-beta binding protein-1. J Cel Biol 2004;165:723–734.

[30] Oklu R, Metcalfe JC, Hesketh TR, et al. Loss of a consensus heparin binding site by alternative splicing of latent transforming growth factor-beta binding protein-1. FEBS Lett 1998;425:281–285.
[31] **Tian F**, **Tong B**, Sun L, et al. N501Y mutation of spike protein in SARS-CoV-2 strengthens its binding to receptor ACE2. Elife 2021;10:e69091.
[32] **Buscemi L**, **Ramonet D**, **Klingberg F**, et al. The single-molecule mechanics of the latent TGF-β1 complex. Curr Biol 2011;21:2046–2054.
[33] Dennler S, Itoh S, Vivien D, et al. Direct binding of Smad3 and Smad4 to critical TGF beta-inducible elements in the promoter of human plasminogen activator inhibitor-type 1 gene. EMBO J 1998;17:3091–3100.
[34] Sun Z, Costell M, Fässler R. Integrin activation by talin, kindlin and mechanical forces. Nat Cel Biol 2019;21:25–31.
[35] Chang JZ-C, Hsieh Y-P, Lin W-H, et al. Activation of transforming growth factor-β1 by thrombin via integrins αvβ1, αvβ3, and αvβ5 in buccal fibroblasts: suppression by epigallocatechin-3-gallate. Head & Neck 2017;39:1436–1445.
[36] **Liu C**, **Wang L**, Xu M, et al. Reprogramming the spleen into a functioning 'liver' in vivo. Gut 2022;71:2325–2336.
[37] **Liao J**, **Chen S**, **Hsiao S**, et al. Therapeutic adenine base editing of human hematopoietic stem cells. Nat Commun 2023;14:207.
[38] Huang P, He Z, Ji S, et al. Induction of functional hepatocyte-like cells from mouse fibroblasts by defined factors. Nature 2011;475:386–389.
[39] Hintze V, Miron A, Moeller S, et al. Sulfated hyaluronan and chondroitin sulfate derivatives interact differently with human transforming growth factor-beta1 (TGF-beta1). Acta Biomater 2012;8:2144–2152.
[40] Kusano M, Mito M. Observations on the fine structure of long-survived isolated hepatocytes inoculated into rat spleen. Gastroenterology 1982;82:616–628.
[41] **Wang Z**, **Tian X**, Wang C, et al. Transforming one organ into another to overcome challenges in tissue engineering. Port Hypertens Cirrhos 2022;1:116–124.
[42] **Lokmic Z**, **Lämmermann T**, Sixt M, et al. The extracellular matrix of the spleen as a potential organiser of immune cell compartments. Semin Immunol 2008;20:4–13.
[43] Meredith Jr JE, Schwartz MA. Integrins, adhesion and apoptosis. Trends Cel Biol 1997;7:146–150.
[44] Zvibel I, Smets F, Soriano H. Anoikis: roadblock to cell transplantation? Cel Transpl 2002;11:621–630.